Advances in Applied Mathematics and Mechanics
Adv. Appl. Math. Mech., Vol. **7**, No. 3, pp. 387-406

DOI: 10.4208/aamm.2012.m42
June 2015

Piecewise Constant Level Set Algorithm for an Inverse Elliptic Problem in Nonlinear Electromagnetism

Xiangyin Kong[1], Zhengfang Zhang[2] and Zhengda Huang[1,*]

[1] *Department of Mathematics, Zhejiang University, Hangzhou 310027, China*
[2] *Department of Mathematics, Hangzhou Dianzi University, Hangzhou 310018, China*

Received 3 December 2012; Accepted (in revised version) 15 September 2014

Abstract. An inverse problem of identifying inhomogeneity or crack in the workpiece made of nonlinear magnetic material is investigated. To recover the shape from the local measurements, a piecewise constant level set algorithm is proposed. By means of the Lagrangian multiplier method, we derive the first variation w.r.t the piecewise constant level set function and obtain the descent direction by the adjoint variable method. Numerical results show the robustness and effectiveness of our algorithm applied to reconstruct some complex shapes.

AMS subject classifications: 65K10, 35Q60, 74M10

Key words: Nonlinear electromagnetism, adjoint variable method, shape reconstruction, piecewise constant level set algorithm.

1 Introduction

In many applications, one needs to find out the flaws in materials nondestructively. Inspired by this, the non-destructive evaluation technique has attracted the eyes of many researchers during the last decades. As one kind of non-destructive evaluation technique, eddy current testing technique [1] has been used for flaw detection. In this paper, we intend to design an algorithm to identify the crack or inhomogeneities in the nonlinear magnetic material like steel from the local measurements of the magnetic induction.

This inverse problem is a problem of shape reconstruction. Similar to general shape recovery problem, there is no information about the interface of the optimal shape as a prior, so we need to have a good mechanism to express the shape and track the evolution of the shape. The level set method was first originally proposed by Osher and Sethian in [2]. For this method, the interface between two adjacent domains is represented by

*Corresponding author.
Email: xiangyinkong@163.com (X. Kong), zhengfangzhang@hdu.edu.cn (Z. Zhang), zdhuang@zju.edu.cn (Z. Huang)

 ©2015 Global Science Press

https://doi.org/10.4208/aamm.2012.m42 Published online by Cambridge University Press

the zero level set of a Lipschitz continuous function. Through the change of this function, this method can easily handle many types of shape and topological changes, such as merging, splitting and developing sharp corners. Due to these merits, it has been used in various areas, such as epitaxial growth [3], inverse problem, optimal design [4], image segmentation [5], structure topology optimization [6] and EIT problem [7]. For the seek of the numerical stability, the level set function is usually chosen as the signed distance function, but at most cases, the level set function after each iteration is not be a signed distance function and is usually re-initialized by solving an ordinary differential equation [8]. In [9], Cimrák et al. used the level set method to represent the shape of the inhomogeneity and evolve the shape by minimizing a functional during the iterative process. In [10, 11], Cimrák also used the level set method for the representation of the interface to solve some inverse problems in thermal imaging and the nonlinear ferromagnetic material. As to the initial value of the level set function, it was reported in [12–14] that the level set method based only on the shape sensitivity may get stuck at shapes with fewer holes than the optimal geometry in some applications such as structure designs. When one wants to use the level set method to solve the practical problem, he can reduce the effects of the initial value of the level set function on the final results in the next two ways. The first way is to choose the shape with enough holes as the initial value. The second one is to introduce the topological derivative into the level set method to let the shape create holes in the iterations [14–18]. To find a good initial value of the level set function, the researchers in [9] proposed the gradient-for-initial approach which is based on the idea that the domain which can drop the value of the cost functional should be the air gap. In that approach, the parameter in smeared-out Heaviside function should be set large enough. The large value of this parameter, however, can cause the oscillation phenomenon. So the parameter in the acquisition of the initial choice of the level set function and the evolving process of level set function should be set separately

Recently, piecewise constant level set method, which is a variant of level set method, was proposed by Lie, Lysaker and Tai in [20–22]. To distinguish these two methods, we call the former one traditional level set method. Unlike the traditional level set method, the interface between two adjacent sub-domains is represented by the discontinuity of a piecewise constant level set function. Compared with traditional level set method, piecewise constant level set method has at least two advantages. One merit is that it can create many small holes automatically without the topological derivatives during the iterative process. Furthermore, it is verified by many numerical examples that the final result is independent of the initial value of the level set function in many numerical tests. And the other one is that the piecewise constant level set method need not to re-initialize the level set function periodically during the evolution process, thus, reduces the computational cost a lot. Since it was proposed, it has been applied in various fields such as image segmentation, elliptic inverse coefficient identification, optimal shape design, electrical impedance tomography and positron emission tomography [19]. Lie, Lysaker and Tai took this method to solve the image segmentation in [20–23] and the elliptic inverse problem and interface motion problem in [24, 25]. Wei and Wang used piecewise

https://doi.org/10.4208/aamm.2012.m42 Published online by Cambridge University Press

constant level set method to solve structural topology optimization in [26]. Zhu, Liu and Wu applied the piecewise constant level set method to solve a class of two-phase shape optimization problems in [27]. Zhang and Cheng proposed a boundary piecewise constant level set method to deal with the boundary control of eigenvalue optimization problems in [28]. In this paper, we intend to use the piecewise constant level set method to represent the shape and recover the exact shape of the crack or the inhomogeneities of nonlinear magnetic material.

Based on the piecewise constant level set method, we propose a piecewise constant level set algorithm to recover the shape of the nonlinear magnetic material problem. We introduce the piecewise constant level set function and convert the constrained optimization problem into an unconstrained one by the Lagrangian multiplier method. In the numerical tests, our algorithm relies little on the initial guess of the level set function. Moreover, our algorithm can reconstruct shape accurately even when the noise level is high.

The rest of this paper is organized as follows. In Section 2, we introduce the piecewise constant level method in brief. In Section 3, we introduce the direct problem and the inverse problem. In Section 4, we describe the deduction of the first variation w.r.t level set function for the objective functional in the unconstrained optimization problem in detail. In Section 5, we present numerical results to show the effectiveness and robustness of piecewise constant level set algorithm.

2 Piecewise constant level set method

We first introduce the piecewise level set method in brief. Suppose that the domain Ω is the union of some sub-domains Ω_i, $i=1,2,\cdots,m$, i.e.,

$$\bar{\Omega}=\bigcup_{i=1}^{m}\Omega_i\cup\bigcup_{i=1}^{m}\partial\Omega_i,$$

where $\partial\Omega_i$ is the boundary of sub-domain Ω_i.

If there exists a function ϕ defined as

$$\phi(\boldsymbol{x})=i,\quad \boldsymbol{x}\in\Omega_i,\quad \text{where } i=1,2,\cdots,m, \tag{2.1}$$

then the interface between two adjoint sub-domains can be identified by the discontinuity of the function ϕ and the characteristic function of the i-th sub-domain Ω_i can be written as

$$\chi_i=\prod_{j=1,j\neq i}^{m}\frac{(\phi-j)}{(i-j)}. \tag{2.2}$$

For the traditional level set method proposed in [2], if ϕ is a level set function, then the expression of χ_i contains the Heaviside function $H(x)$, which is defined as below:

$$H(x)=\begin{cases}1, & x\geq 0,\\ 0, & x<0.\end{cases} \tag{2.3}$$

https://doi.org/10.4208/aamm.2012.m42 Published online by Cambridge University Press

Since $H(x)$ is not differentiable at 0, it is often replaced by smooth functions which contain some parameters in [25]. Sometimes the parameters in the replaced smooth functions can cause difficulties in the result analysis, such as the convergence of the level set ϕ in [9]. For the piecewise constant level set method, we do not encounter this kind of problems.

If ϕ is defined as in (2.1), then it holds that

$$K(\phi)=0 \quad \text{in } \Omega, \tag{2.4}$$

where the function K is defined as

$$K(\phi)=(\phi-1)(\phi-2)\cdots(\phi-m)=\prod_{i=1}^{m}(\phi-i). \tag{2.5}$$

It should be pointed out that if Eq. (2.4) holds, then every point $\boldsymbol{x}\in\Omega$ is in one and only one sub-domain. In other words, there is no vacuum and overlap between two different sub-domains.

For any piecewise smooth function $f(\boldsymbol{x})$ that coincides with $f_i(\boldsymbol{x})$ in Ω_i, it can be written as

$$f(\boldsymbol{x})=\sum_{i=1}^{m}f_i(\boldsymbol{x})\chi_i(\phi(\boldsymbol{x})), \tag{2.6}$$

where $\phi(\boldsymbol{x})$ is defined in (2.1).

3 Direct problem and inverse problem

We first introduce the quasi-linear partial differential equation which will be used in this paper.

This equation is defined as

$$\begin{cases} \nabla\cdot(v(\boldsymbol{x},|\nabla A|^2)\nabla A)=J & \text{in } \Omega, \\ A=0 & \text{on } \partial\Omega, \end{cases} \tag{3.1}$$

where $\Omega\subset\mathbb{R}^2$ is a bounded domain with C^1 boundary, the symbol J denotes a suitable function defined in Ω and the function $v:\Omega\times\mathbb{R}\to\mathbb{R}$ is defined as

$$v(\boldsymbol{x},s)=\begin{cases} v_1(s), & \boldsymbol{x}\in D, \\ v_2(s), & \boldsymbol{x}\in\Omega\backslash D, \end{cases} \tag{3.2}$$

where $D\subset\Omega$, v_1, v_2 are two functions determined by the specific practical applications.

Eq. (3.1) can model many industrial and physical applications. When both v_1 and v_2 are constant functions, it is the elliptic inverse problem in [24]. When v_1 and v_2 are both linear ones, it characterizes the electric impendence tomograph problem [29]. Since the material in this paper is nonlinear magnetic, we use the nonlinear model, which is more robust and able to reconstruct the shape of the crack or inhomogeneities even when the linear model is not [9]. In this model, v_2 is a nonlinear function.

https://doi.org/10.4208/aamm.2012.m42 Published online by Cambridge University Press

Since we need to solve the direct problem in each iteration, we next present the direct problem in detail. The direct problem is to obtain the quantity A when the variable v, the domain D and the function J are given. In this paper, our goal is to design a numerical scheme to identify the crack or the inhomogeneity in the workpiece which is made of nonlinear magnetic material. In this case, the function J denotes the induced current density, the quantity A denotes the only nonzero component of the vector potential $\boldsymbol{A}$ which is perpendicular to the xy-plane. According to the physical knowledge, the magnetic induction $\mathbf{B}$ is

$$\mathbf{B}=\Big(\frac{\partial A}{\partial y},-\frac{\partial A}{\partial x},0\Big)^T. \tag{3.3}$$

Since A is defined on a subregion of $\mathbb{R}^2$, we obtain

$$|\mathbf{B}|=|\nabla A|.$$

After introducing two symbols μ_1 and μ_2 to denote the magnetic permeability of the air and the nonlinear magnetic material, we define the functions v_1 and v_2 as the reciprocal of the two functions μ_1 and μ_2, respectively, i.e., $v_1=1/\mu_1$ and $v_2=1/\mu_2$. As to μ_2, due to the nonlinear magnetic property of the material, it depends on $|\nabla A|$. Usually, the function $\mu_2(s)$ is monotonically increasing on the interval $[0,s_{\max}]$ and is monotonically decreasing on the interval $[s_{\max},+\infty]$, where $s_{\max}$ is a number determined by the property of the magnetic nonlinear material.

With the piecewise constant level set method, the function $v(\boldsymbol{x})$ can be formulated as

$$v(\boldsymbol{x})=v_1(2-\phi)+v_2(\phi-1). \tag{3.4}$$

By (3.4), the weak form of the Eq. (3.1) can be written as

$$\int_\Omega [v_1(|\nabla A|^2)(2-\phi)+v_2(|\nabla A|^2)(\phi-1)]\nabla A\cdot\nabla\varphi d\boldsymbol{x}=\int_\Omega J\varphi d\boldsymbol{x},\quad \forall\varphi\in W_0^{1,2}(\Omega). \tag{3.5}$$

The existence and uniqueness of the solution to the Eq. (3.5), have been proved in [30, 31]. To ensure the existence and uniqueness of the solution to Eq. (3.5), we adopted the assumptions in [9] which are listed as below:

A1 The function v_i is non-decreasing;

A2 $\lim_{s\to 0}v_i(s)=v_{\min}>0$;

A3 $\lim_{s\to\infty}v_i(s)=v_{\max}>0$ and define $v(s)=v_{\max}$ for $s=\infty$;

A4 v_i is differentiable with well-defined derivatives v_i' satisfying

$$v'_{\min}\le v_i'\le v'_{\max},$$

where $i=1,2$.

https://doi.org/10.4208/aamm.2012.m42 Published online by Cambridge University Press

In order to let the function μ_2 satisfy the non-decreasing property in the assumption **A1**, we set the function J large enough. As to the solution to Eq. (3.1), we consider it as the solution to the following nonlinear operator equation

$$G(A)=J,$$

where G is an operator defined in the space $W_0^{1,2}(\Omega)$ and takes values in $W_0^{1,2}(\Omega)$. To solve this nonlinear operator equation, we first choose an initial guess A_0 of A, and use the Newton-Raphson algorithm to update A, i.e.,

$$A_{i+1}=A_i-[DG(A_i)]^{-1}(G(A_i)-J),$$

where $i=1,2,\cdots$.

Now we introduce the inverse problem. When v_1 and v_2 are given, the inverse problem is to reconstruct the actual shape of D from the measurement data $\overline{\mathbf{M}}$ of magnetic induction in a given subset $\Gamma\subset\Omega$. Under the framework of the piecewise constant level set method, the problem is to find a piecewise constant function ϕ to approximate the exact level set function which can represent the actual composition of the workpiece (during the iterative process, the level set function ϕ may be not a piecewise constant one). In order to distinguish these two functions, we denote by ϕ_{exact} the exact level set function here and afterward. For our work, $\Gamma=\Omega$.

When the level set function ϕ and the data $\overline{\mathbf{M}}$ on Γ are given, we use the following functional

$$F_1(\phi)=\frac{1}{2}\int_\Gamma|\nabla A(\phi)-\overline{\mathbf{M}}|^2d\boldsymbol{x} \tag{3.6}$$

to measure the misfit between ϕ and ϕ_{exact}, where $\overline{\mathbf{M}}=(-\overline{B}_2,\overline{B}_1)^T$ with $\overline{B}_1$ and $\overline{B}_2$ being the x-axis and y-axis component of $\mathbf{B}$. Obviously, the smaller the value of F_1 is, the more close the level set ϕ is to ϕ_{exact}. Thus the inverse problem is converted into the following optimization problem

$$\min_\phi F_1(\phi)\ \text{ subject to } K(\phi)=0, \tag{3.7}$$

where $K(\phi)$ is defined in (2.5).

4 Algorithm

In this section, we will introduce our piecewise constant level set algorithm for this inverse problem.

We first give the deduction of the gradient of F_1. Introducing two symbols DF_1 and $\delta_h g$ to denote the gradient of F_1 and the Gâteaux of g with respect to ϕ in the direction h, we give the deduction of $\delta_h F_1$. According to the definition, it can be expressed as

$$\delta_h F_1=\lim_{\epsilon\to0}\frac{F_1(\phi+\epsilon h)-F_1(\phi)}{\epsilon}=\int_\Gamma\nabla\delta_h A\cdot(\nabla A-\overline{\mathbf{M}})d\boldsymbol{x}, \tag{4.1}$$

https://doi.org/10.4208/aamm.2012.m42 Published online by Cambridge University Press

where $\nabla\delta_h A$ will be given below.

Differentiating both sides of Eq. (3.5) with respect to ϕ, we obtain the following sensitivity equation

$$\int_\Omega \delta_h[v(\boldsymbol{x},|\nabla A|^2)]\nabla A\cdot\nabla\varphi d\boldsymbol{x}+\int_\Omega v(\boldsymbol{x},|\nabla A|^2)\nabla\delta_h A\cdot\nabla\varphi d\boldsymbol{x}=0. \tag{4.2}$$

Since A is completely determined by the level set function ϕ when J, v_1 and v_2 are given, from (3.4), the integral part of the first term in (4.2) can be sorted as

$$\begin{aligned}\delta_h[v(\boldsymbol{x},|\nabla A|^2)]=&(v_2(|\nabla A|^2)-v_1(|\nabla A|^2))h\\&+(2-\phi)\delta_h[v_1(|\nabla A|^2)]+(\phi-1)\delta_h[v_2(|\nabla A|^2)]\\=&(v_2(|\nabla A|^2)-v_1(|\nabla A|^2))h\\&+2((2-\phi)v_1'(|\nabla A|^2)+(\phi-1)v_2'(|\nabla A|^2))\nabla A\cdot\nabla\delta_h A.\end{aligned} \tag{4.3}$$

Substitute (4.3) into (4.2) and simplify the equation, the sensitivity equation (4.2) can be written as

$$\begin{aligned}&\int_\Omega (v_2(|\nabla A|^2)-v_1(|\nabla A|^2))h\nabla A\cdot\nabla\varphi d\boldsymbol{x}\\=&-\int_\Omega 2((2-\phi)v_1'(|\nabla A|^2)+(\phi-1)v_2'(|\nabla A|^2))\nabla A\cdot\nabla\delta_h A\nabla A\cdot\nabla\varphi d\boldsymbol{x}\\&-\int_\Omega v(\boldsymbol{x},|\nabla A|^2)\nabla\delta_h A\cdot\nabla\varphi d\boldsymbol{x}.\end{aligned} \tag{4.4}$$

As to the computation of $\nabla\delta_h A$, it could be deduced by the adjoint variable method which was used in many problems [32–37]. Specifically, we take the following steps to avoid the direct computation of $\nabla\delta_h A$.

Firstly, we determine the solution to the following equation which we will denote p afterward

$$\begin{aligned}&\int_\Omega 2((2-\phi)v_1'(|\nabla A|^2)+(\phi-1)v_2'(|\nabla A|^2))\nabla p\cdot\nabla A\nabla A\cdot\nabla\psi d\boldsymbol{x}\\&+\int_\Omega v(\mathbf{x},|\nabla A|^2)\nabla p\cdot\nabla\psi d\boldsymbol{x}=\int_\Gamma \nabla\delta_h A\cdot(\nabla A-\overline{\mathbf{M}})d\boldsymbol{x}.\end{aligned} \tag{4.5}$$

Secondly, by letting the test function for the variable ψ and ϕ in (4.4) and (4.5) being p and $\delta_h A$, respectively, we can get the following equation

$$-\int_\Omega (v_2(|\nabla A|^2)-v_1(|\nabla A|^2))h\nabla A\cdot\nabla\psi d\boldsymbol{x}=\int_\Gamma \nabla\delta_h A\cdot(\nabla A-\overline{\mathbf{M}})d\boldsymbol{x}. \tag{4.6}$$

By comparing Eq. (4.1) with Eq. (4.6), we obtain

$$\delta_h F_1=-\int_\Omega (v_2(|\nabla A|^2)-v_1(|\nabla A|^2))h\nabla A\cdot\nabla p d\boldsymbol{x}. \tag{4.7}$$

https://doi.org/10.4208/aamm.2012.m42 Published online by Cambridge University Press

After deriving the formula of $\delta_h F_1$, we simply obtain DF_1 by simply projecting $(v_2(|\nabla A|^2)-v_1(|\nabla A|^2))\nabla A\cdot\nabla p$ onto the finite element space $W_0^{1,2}(\Omega)$ by solving the following equation

$$-\int_\Omega (v_2(|\nabla A|^2)-v_1(|\nabla A|^2))\nabla A\cdot\nabla p\varphi d\boldsymbol{x}=\int_\Omega DF_1\varphi d\boldsymbol{x}. \tag{4.8}$$

In the numerical tests, it often comes out that the level set function ϕ can not approximate ϕ_{exact} correctly at the boundary of Ω. To approximate the function ϕ_{exact} more accurately, we introduce a Tikhonov stabilizing term $\int_\Omega|\nabla\phi|^2 d\boldsymbol{x}$, then the constrained optimization problem (3.7) becomes

$$\min_\phi F \ \text{ subject to } \ K(\phi)=0, \tag{4.9}$$

where $F=F_1+\alpha\int_\Omega|\nabla\phi|^2 d\boldsymbol{x}$ and the coefficient α is a positive real number.

Similar to the deduction of DF_1, the gradient DF of F is calculated by solving the following equation

$$\int_\Omega (v_2(|\nabla A|^2)-v_1(|\nabla A|^2))\nabla A\cdot\nabla p\varphi d\boldsymbol{x}+2\alpha\int_\Omega\nabla\phi\cdot\nabla p\varphi d\boldsymbol{x}=\int_\Omega DF\varphi d\boldsymbol{x}. \tag{4.10}$$

In this paper, we use the Lagrangian multiplier method to convert the problem (4.9) into the following unconstrained optimization problem

$$L(\phi)=F(\phi)+\int_\Omega l_1(x)K(\phi)d\boldsymbol{x}, \tag{4.11}$$

where l_1 is the Lagrangian multiplier, a l^2-integrable function defined on the domain Ω.

According to the general theory of optimization, the level set function ϕ that we seek is the saddle point of the functional $L(\phi)$, that is,

$$\frac{\partial L}{\partial\phi}=\frac{\partial F}{\partial\phi}+l_1(2\phi-3)=0,\quad \frac{\partial L}{\partial l_1}=K(\phi)=0. \tag{4.12}$$

By multiplying two sides of Eqs. (2.4) by $(2\phi-3)$ and making use of the constraint $(\phi-1)(\phi-2)=0$, we get the formula to update the multiplier

$$l_1=-(2\phi-3)\frac{\partial F}{\partial\phi}. \tag{4.13}$$

Substituting (4.13) into (4.12), we have

$$\frac{\partial L}{\partial\phi}=-4(\phi-1)(\phi-2)\frac{\partial F}{\partial\phi}. \tag{4.14}$$

We introduce the artificial time variable t and update the level set function ϕ according to the following scheme

$$\begin{cases}\dfrac{\partial\phi}{\partial t}=-\dfrac{\partial L}{\partial\phi} & \text{in } \Omega\times\mathbf{R}^+,\\ \phi(\boldsymbol{x},t)=\phi_0(\boldsymbol{x}) & \text{in } \Omega,\end{cases} \tag{4.15}$$

https://doi.org/10.4208/aamm.2012.m42 Published online by Cambridge University Press

until the level set function ϕ satisfy $\partial\phi/\partial t=0$.

To discretize (4.15), we use the forward Euler scheme

$$\phi_{k+1}=\phi_k-\Delta t_k\frac{\partial L}{\partial\phi}\Big|_{\phi=\phi_k},\quad k=0,1,2,\cdots. \tag{4.16}$$

During the iteration process, for the seek of numerical stability, we let the time step Δt_k satisfy the Courant-Friedrichs-Lewy condition

$$\Delta t_k=\sigma h\Big/\max_{x\in\Omega}\Big|\frac{\partial L}{\partial\phi}(\phi_k)\Big|, \tag{4.17}$$

where $\sigma\in(0,1)$ and h is mesh size.

We now give the choice of ϕ_0 and the projection used in the iteration process. We let ϕ_0 be a function whose value at every point is neither 1 nor 2, or let ϕ_0 be a constant function and the constant is a number between 1 and 2 (1 and 2 are excluded). Considering the fact that the value of the final ϕ at every point $\mathbf{x}\in D$ should be either 1 or 2, we project ϕ in the following way:

$$P_{\{1,2\}}\phi=\begin{cases}1, & \phi<1,\\ 2, & \phi>2,\\ \phi(\mathbf{x}), & \text{otherwise},\end{cases} \tag{4.18}$$

after updating ϕ by (4.16) at each step.

From Eq. (4.14), the gradient $\partial L/\partial\phi$ is equal to 0 when the value of ϕ is either 1 or 2. This sometimes causes the iterative process unable to start or proceed, thus we exclude 1 and 2 from being the candidates of the constant for ϕ_0. In order to avoid this phenomenon in the iteration process, we count the number N of the points at which the function ϕ take 1 or 2 after projecting the level set function ϕ by $P_{1,2}$. If the number N is equal to N_T which denotes the number of the total points, we stop and exit the iterative process.

In our numerical tests, there is no such case that the iteration process stops for the reason that $N=N_T$. Considering the fact that F_1 becomes smaller as the iteration proceeds, we introduce a variable *osci* to denote the times that the F_1 oscillates and exit the iterative process when *osci* reaches a given number.

Now we will present the piecewise constant level set algorithm (PCLSA).

Remark 4.1. After exiting the iterative process, the value of the level set function ϕ at every point $\boldsymbol{x}\in\Omega$ usually doesn't satisfy the constraint $(\phi-1)(\phi-2)=0$. To make ϕ satisfy the constraint, we project ϕ as below:

$$P_u(\phi)=\begin{cases}1, & \phi\le 1.5,\\ 2, & \phi>1.5,\end{cases} \tag{4.19}$$

after exiting the iteration process.

https://doi.org/10.4208/aamm.2012.m42 Published online by Cambridge University Press

Algorithm 1. PCLSA.

Initialize ϕ_0 as a suitable function, $F_{1,-1}$=10000, $osci$=0 and N=0, Compute N_T. For k=0,1,2,$\cdots$,

Step 1 Use ϕ_k to update $v: v_k(\boldsymbol{x}) = v_{1,k}(2-\phi_k)+v_{2,k}(\phi_k-1)$ and obtain A_k and ∇A_k by solving Eq. (3.5) with the Newton-Raphson method.

Step 2 Compute $F_{1,k}$ by (3.6). let $osci$:=$osci$+1 if $F_{1,k}>F_{1,k-1}$. If $osci$ is equal to the predetermined value, exit the iterative process; Otherwise, go to Step 3.

Step 3 Solve the Eq. (4.10) to compute the gradient of F_1 according to ϕ_k and ∇A_k, and update $(\partial L/\partial\phi)|\phi_k$.

Step 4 Set Δt_k by (4.17) and use the scheme (4.16) to update the level set function ϕ.

Step 5 Project ϕ by (4.18). Check the projected ϕ and obtain N. Exit the iterative process if $N=N_T$. Or else, set $k:=k+1$ and $\phi_k=\phi$, go to Step 1.

5 Numerical results

In this section, four examples are solved by Algorithm 1 (PCLSA). The workpiece we studied in the numerical tests is made of the hard steel and possibly contains the crack which is filled with the air. The magnetic permeability of air is close to 1, i.e., $\mu_1=1$, so $v_1=1$. For the function v_2, which is relevant to the magnetic permeability of the hard steel, is defined as

$$v_2(s)=d_1+\frac{c_1 s^{b_1}}{a_1^{b_1}+s^{b_1}},$$

where the concrete values for the four variables in v_2 are set the same as [9]:

$$a_1=0.5,\quad b_1=4,\quad c_1=3,\quad d_1=0.2.$$

For all examples, the domain $\Omega=[-0.5,0.5]\times[-0.5,0.5]$ and all the numerical tests are run on the PC with Intel Core 2 Duo 2.10GHz processor and 2GB RAM by the software Matlab 2010b. When solving the Eqs. (3.5) and (4.10), we divide the domain Ω into some rectangles with the size $h_x=h_y=h=1/dim$, where dim is the number of rectangles in the x-direction. For the measurement data $\overline{\mathbf{M}}$, we generate it in the following steps: we first find a level set function ϕ_{exact} to represent the shape of D accurately, then solve Eq. (3.5) with the Newton-Raphson algorithm to obtain the solution A_{exact}, finally assign ∇A_{exact} to $\overline{\mathbf{M}}$. In order to see the closeness of the function ϕ to ϕ_{exact}, we call the built-in "contour" command in Matlab to plot the interface between two sub-domains after the test. For the command "contour", we set the parameter for the number of the contour line as 1 and choose the red-solid-line and the blue-dotted-line to denote the interface between two sub-domains represented by ϕ_{exact} and ϕ, respectively. In the figures that depict the evolution of the level set function, the red part and the blue part represent the hard steel and the air, respectively. In the figures that depict the evolution of the level set function, the red part and the blue part represent the hard steel and the air, respectively. In some

https://doi.org/10.4208/aamm.2012.m42 Published online by Cambridge University Press

figures, the shapes of some graphics don't look like shapes they should be. For instance, the shape of the circle in Example 5.1 is more like an octagon. In order to measure the misfit between the computed ϕ and ϕ_{exact} precisely, we count the number of the points where two functions take different values.

In this section, we do two groups of numerical tests to show the effectiveness and robustness of PCLSA. The first group of tests are based on the measurement data $\overline{\mathbf{M}}$ without noise. In order to show the flexibility of the choice of the initial guess of ϕ, we set the function ϕ as some different initial values and observe the final shapes. The second group of tests are based on the measurements data $\overline{\mathbf{M}}$ with a certain level of noise. As to the robustness of PCLSA, our algorithm can reconstruct the shape precisely when the noise level is up to 15%, which is superior to the algorithm in [9].

Example 5.1. In this example, We use the same configuration as in [9]. The exact shape of the domain D is a circle with the center $(0.2,0.15)$ and the radius 0.1. And the induced current density J is defined as follows:

$$J(x,y)=\begin{cases} J_1, & y>0.4, \\ -J_1, & y<-0.4, \\ 0, & \text{otherwise}, \end{cases} \tag{5.1}$$

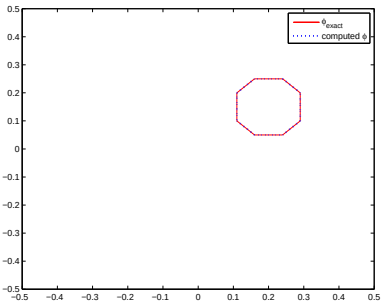
where $J_1=500$. This choice of J describes the case that the workpiece is wrapped by the wires.

For this test, we set $dim=50$, $\sigma=0.9$ and $\alpha=0.001$. The initial value of the level set function is chosen as $\phi_0=1.5$ and the upper bound of $osci$ is 10. The iterative process stops after 304 steps. We present the results in Fig. 1.

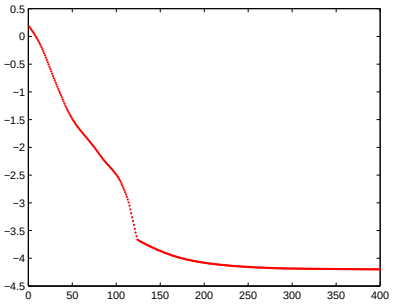
In Fig. 1(a), the red solid line and the blue dotted line coincide, that is to say, PCLSA can identify the shape of the air gap completely. In this test, the two functions, ϕ and ϕ_{exact}, take the same value at every point $\boldsymbol{x}\in\Omega$. Fig. 1(b) shows the change of F_1 with respect to the number of iterations. From Fig. 1(b), we can see that the value of F_1 first becomes smaller, but doesn't become smaller any more after 300 steps. So it is reasonable for us to choose $osci=10$. Fig. 1(c) to Fig. 1(f) show the evolution of the function ϕ and the interface. During the iterative process, the values of ϕ at the points of Ω develop towards to our expectation except four corner points. As the increase of the number of iterations, the values of ϕ at these four points first become small, which is away from our expectation, but becomes large after some steps. In Fig. 2, the values of the level set function ϕ at the four corner points and some points at the boundary of Ω are 1 instead of 2. By comparing with the picture of ϕ after 300 steps (see Fig. 1(f) and Fig. 2), we can see that it's the effects of the regularization to let the values of ϕ at four points become large.

Example 5.2. In this example, the shape of the air gap in the workpiece is non-convex, which is more like a shrimp. The current density function J is defined as (5.1) with the constant J_1 equal to 500. This numerical test describes the case that the workpiece is all wrapped with the wires.

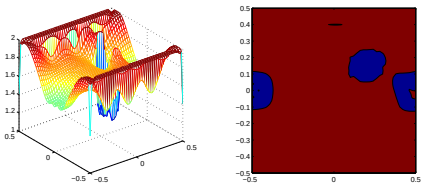
https://doi.org/10.4208/aamm.2012.m42 Published online by Cambridge University Press



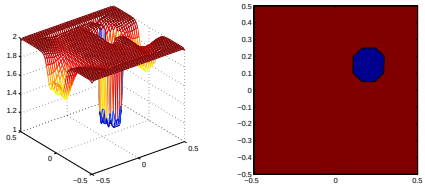
(a) The interfaces represented by ϕ_{exact} and ϕ



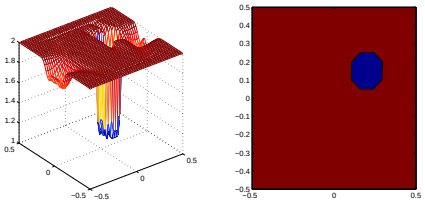
(b) The value of $\log F_1 / \log 10$



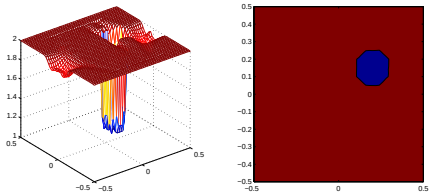
(c) Step 75



(d) Step 150



(e) Step 225



(f) Step 300

Figure 1: Numerical results for Example 5.1. (a) The final reconstruction of ϕ. (b) The change of the value of F_1 vs. the number of iterations. (c)-(f) The evolution of ϕ and the interface.

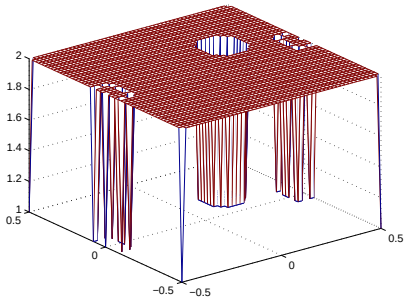


Figure 2: The figure of computed ϕ without regularization.

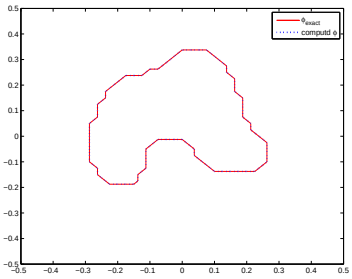
https://doi.org/10.4208/aamm.2012.m42 Published online by Cambridge University Press

In this test, we set some variables as follows:

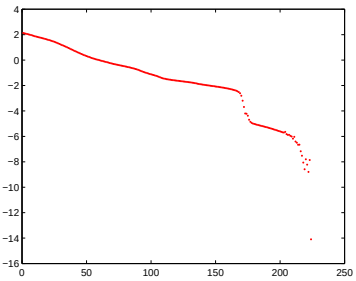
$$dim = 40, \quad \alpha = 0.001, \quad \sigma = 0.9.$$

The initial guess of ϕ and the upper bound of *osci* are chosen as $\phi_0 = 1.5$ and 15, respectively. The iterative process stops after 212 iterations. We present the numerical results in Fig. 3.

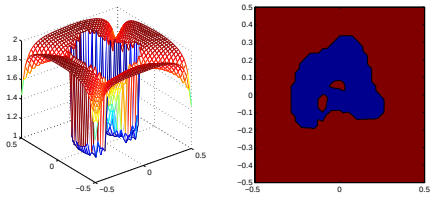
In Fig. 3(a), the red solid line coincides with the blue dotted one. And the number of the points where ϕ and ϕ_{exact} take different values is 0. That is, the algorithm can identify the shape of D accurately. Fig. 3(b) depicts the change of F_1 with respect to the number of iterations. In Fig. 3(b), unlike Example 5.1, the value of F_1 is below 10^{-11} after some oscillations. Before exiting the iterative process, the times that the value of F oscillates do not exceed 15, so it's reasonable to choose the upper bound of *osci* to be 15. Fig. 3(c) to



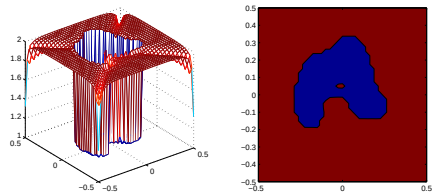
(a) The interfaces represented by ϕ_{exact} and ϕ



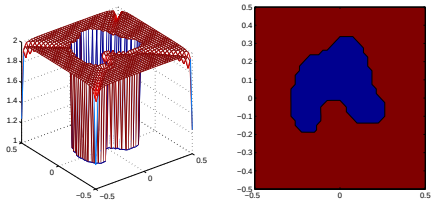
(b) The value of $\log F_1 / \log 10$



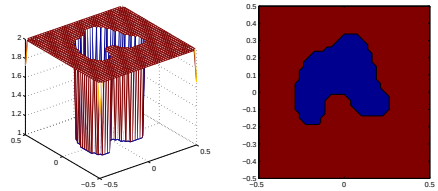
(c) Step 50



(d) Step 100



(e) Step 150



(f) Step 200

Figure 3: Numerical results for Example 5.2. (a) The final reconstruction of ϕ. (b) The change of the value of F_1 vs. the number of iterations. (c)-(f) to show the evolution of ϕ and the interface.

https://doi.org/10.4208/aamm.2012.m42 Published online by Cambridge University Press

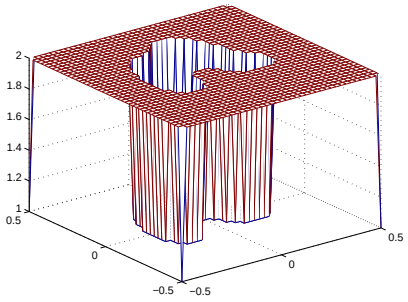


Figure 4: The figure of ϕ without regularization.

Fig. 3(f) describe the evolution of ϕ and the interface. Similar to the evolution of the level set function ϕ in the Example 5.1, as the increase of the number of iterations, the values of ϕ at four corners first become smaller then start to increase to 2. In Fig. 4, the values of ϕ at four points of Ω are 1. Thus we can conclude that it is the effects of the regularization to pull the values of ϕ at these points back to 2.

Example 5.3. In this example, in order to test the ability of identifying the crack that is disconnected, we let the crack be the union of two circles and an ellipse. The current density function is chosen as $J=500$.

In this test, the variables are chosen as follows:

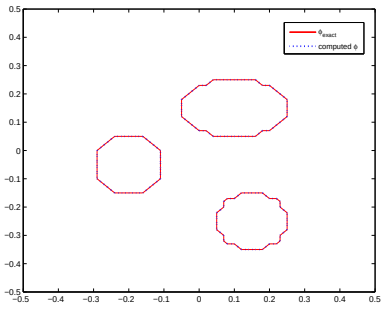
$$dim=50, \quad \alpha=0.001, \quad \sigma=0.9.$$

The initial value of the level set function and the upper bound of *osci* are $\phi_0=1.5$ and 10, separately. The iterative process stops after 306 steps. We present the numerical results in Fig. 5.

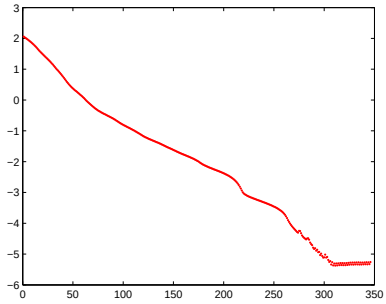
In Fig. 5(a), the interfaces between steel and air, represented by the red solid line and the blue dotted line, coincide. And the number of the points which ϕ and ϕ_{exact} take different values is 0. Fig. 5(b) depicts the change of F_1 with respect to the number of iterations. In Fig. 5(b), the value of F_1 first decreases and then oscillates in the last few steps. So it is reasonable for us to choose 10 as the upper bound of *osci*. Fig. 5(c) to Fig. 5(f) describe the evolution of ϕ and the interface. As the increase of the number of iterations, the values of ϕ at four corners first become smaller then start to increase to 2. In Fig. 6, the values of ϕ at four points of Ω are 1. Thus we can conclude that it is the effects of the regularization term to pull the values of ϕ at these points to 2.

Compared with the algorithm in [9], PCLSA takes much less steps, but reconstructs a more accurate shape. In [9], it takes 574 iteration steps to stop the algorithm. In our PCLSA, we only need half of that iterations, that is, totally 307 iterations to stop the algorithm. Moreover, with more iterations in [9] the final reconstruction shape still deviates a lot from the exact shape. In our final result (see Fig. 5), however, there is no deviations at all.Thus PCLSA performs better than the algorithm in [9] for this example.

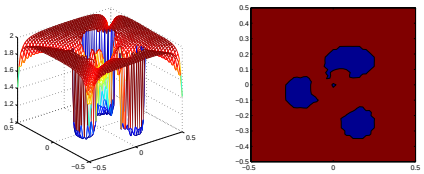
https://doi.org/10.4208/aamm.2012.m42 Published online by Cambridge University Press



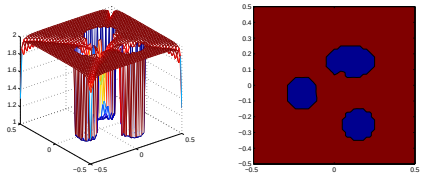
(a) The interfaces represented by ϕ_{exact} and ϕ



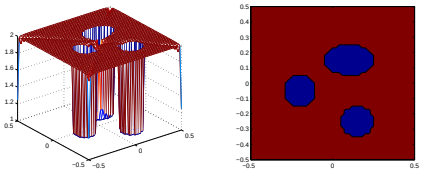
(b) The value of $\log F_1/\log 10$



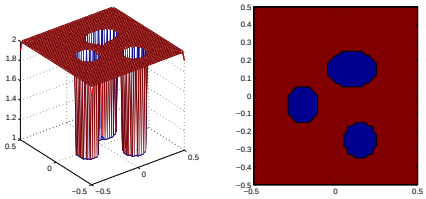
(c) Step 75



(d) Step 150



(e) Step 225



(f) Step 300

Figure 5: Numerical results for Example 5.3. (a) The final reconstruction of ϕ. (b) The change of the value of F_1 vs. the number of iterations. (c)-(f) to show the evolution of ϕ and the interface.

In order to show the flexibility of the initial guess of ϕ, we assign different values to ϕ_0 and compare the final results. we set ϕ_0 to be different constants, that is, 1.2, 1.4, 1.7, 1.9, respectively, and present the final results in Fig. 7. For these four different values of ϕ_0, the interfaces represented by ϕ and ϕ_{exact} coincide and the number of the points where ϕ and ϕ_{exact} take different value is 0. This indicates that our algorithm can identify the shape exactly. Furthermore, we choose a more general function as the initial value of ϕ and also observe the final interface. The general function is $\phi(x) = 1 + rand(x)$ where $rand(x)$ can produce pseudo-random values between 0 and 1. We present the numerical results in Fig. 8, where the interfaces represented by ϕ and ϕ_{exact} coincide.

From the above observation, PCLSA relies little on the initial value of the level set function. Thus, we need not to put too much attentions on the initial guess of ϕ in our PCLSA for the nonlinear electromagnetism recovery problems.

https://doi.org/10.4208/aamm.2012.m42 Published online by Cambridge University Press

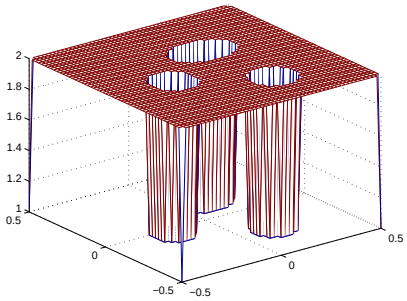
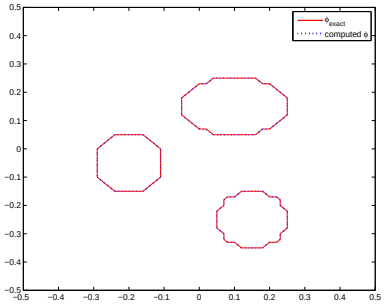
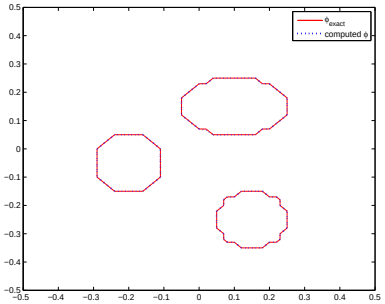


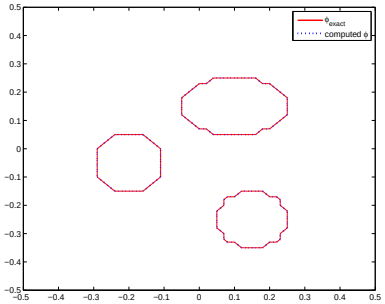
Figure 6: The figure of ϕ without regularization.



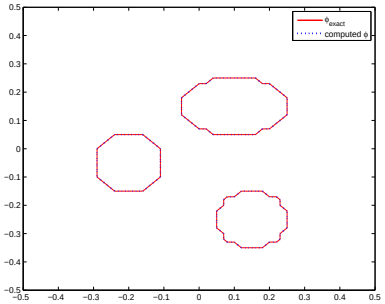
(a) The final result for $\phi_0 = 1.2$



(b) The final result for $\phi_0 = 1.4$



(c) The final result for $\phi_0 = 1.7$



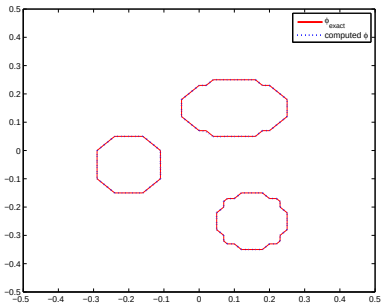
(d) The final result for $\phi_0 = 1.9$

Figure 7: The final recovery interfaces of different values of ϕ_0.

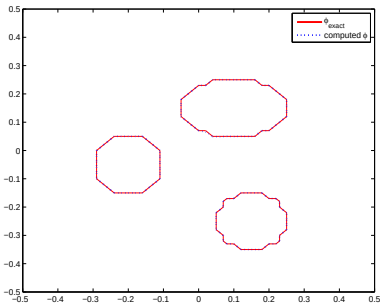
Example 5.4. To test the robustness of PCLSA, we use the measurement data of $\overline{\mathbf{M}}$ with a certain level of noise. For this test, we use the same case in Example 5.2 except that the measurement data of $\overline{\mathbf{M}}$ is polluted by the certain level of noise, 5%, 10%, 15% and 20%.

In this test, $dim = 50$. We set $\phi_0 = 1.5$, the upper bound of $osci$ to be 10, $\alpha = 0.1$ and $\sigma = 0.9$. For different noise level cases, the final results are shown in Fig. 9. When the noise level is under 15%, the PCLSA reconstructs the shape of D completely. That is,

https://doi.org/10.4208/aamm.2012.m42 Published online by Cambridge University Press

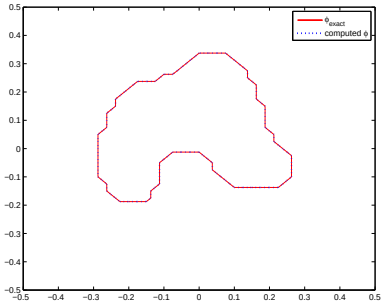


(a) The final result for for Case 1

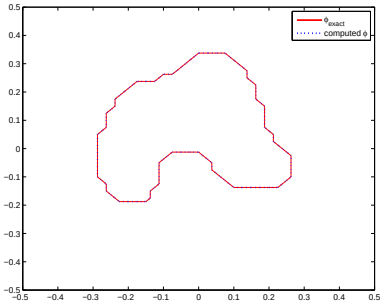


(b) The final result for Case 2

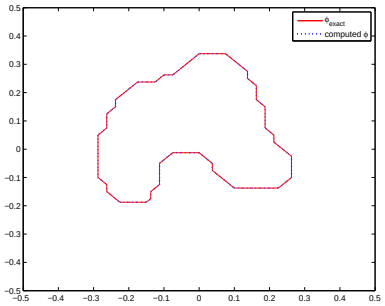
Figure 8: The final recovery interfaces of two cases of rand initial guesses: $\phi_0(x)=1+rand(x)$.



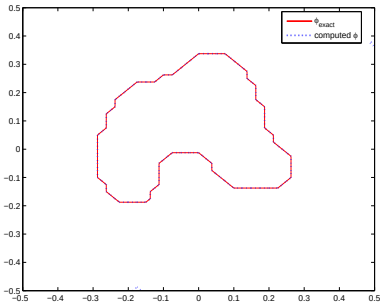
(a) The final result for 5% noise



(b) The final result for 10% noise



(c) The final result for 15% noise



(d) The final result for 20% noise

Figure 9: The final recovery interfaces of different noise levels in Example 5.4.

in our numerical test, the two functions ϕ and ϕ_{exact} take the same value at every point $x\in\Omega$. But when the noise level is up to 20%, though the interface between the steel and air represented by ϕ is recovered, there are some flaws at the interface between D and $\Omega\backslash D$ (some blue points). For the range of σ, the interval $0.6\sim0.9$ is shown by our numerical tests to be not a bad choice.

https://doi.org/10.4208/aamm.2012.m42 Published online by Cambridge University Press

However, σ affects the iteration steps in our PCLSA. The larger σ is, the less steps the algorithm takes. But at high noise level, the reconstructed shape is better when the value of σ is smaller.

6 Conclusions

In this paper, we propose a piecewise constant level set algorithm for the nonlinear electromagnetism inverse problem. In our numeric test, our PCLSA do not rely on the initial guess of the level set function ϕ, and can reconstruct the shape of Ω exactly even when the noise level is high. Our PCSLA is quite effective and robust to solve a kind of nonlinear inverse problems.

Acknowledgments

We express our gratitude to Doctor Ivan Cimrâk for his prompt and comprehensive answer to our problems. This work is supported by Natural Science Foundation of Zhejiang Province, China (No. LY12A01023, LQ12A01001), National Natural Science Foundation of China (No. 11201106, 11471285).

References

[1] S. Giguère, B. Lepine and J. Dubois, *Pulsed eddy current technology: characterizing material loss with gap and lift-off variations*, Research in Nondestructive Evaluation, 13 (2001), pp. 119–129.
[2] S. Osher and J. A. Sethian, *Fronts propagating with curvature dependent speed: Algorithms based on Hamilton-Jacobi formulations*, J. Comput. Phys., 79 (1988), pp. 12–49.
[3] S. Chen, B. Merriman, M. Kang, R.-E. Caflisch, C. Ratsch, L.-T Cheng, M. Gyure, R.-P. Fedkiw, C. Anderson and S. Osher, *A level set method for thin film epitaxial growth*, J. Comput. Phys., 167 (2001), pp. 475–500.
[4] M. Burger and S. Osher, *A survey on level set methods for inverse problems and optimal design*, Euro. J. Appl. Math., 16 (2005), pp. 263–301.
[5] L. A. Vese and T. F. Chan, *A multiphase level set framework for image segmentation using the mumford and shah model,* Int. J. Comput. Vis., 50 (2002), pp. 271–293.
[6] M. Y. Wang, X. Wang and D. Guo, *A level set method for structural topology optimization,* Comput. Methods Appl. Mech. Eng., 192 (2003), pp. 227–246.
[7] N. M. Tanushev and L. A. Vese, *A Piecewise-constant binary model for electrical impedance tomography,* Inverse Probl. Imag., 2 (2007), pp. 423–435.
[8] M. Sussman, P. Smereka and S. Osher, *A level set approach for computing solutions to incompressible two-phase flow,* J. Comput. Phys., 114 (1994), pp. 146–159.
[9] I. Cimrák and R. V. Keer, *Level set method for the inverse elliptic problem in nonlinear electromagnetism*, J. Comput. Phys., 229 (2010), pp. 9269–9283.
[10] I. Cimrák, *Inverse thermal imaging inmaterials with nonlinear conductivity bymaterial and shape derivative method,* Math. Methods Appl. Sci., 34 (2011), pp. 2303–2317.

https://doi.org/10.4208/aamm.2012.m42 Published online by Cambridge University Press

[11] I. CIMRÁK, *Material and shape derivative method for quasi-linear elliptic systems with applications in inverse electromagnetic interface problems,* SIAM J. Numer. Anal., 50 (2012), pp. 1086–1110.
[12] G. ALLAIRE, F. JOUVE AND A.-M. TOADER, *A level-set method for shape optimization,* C. R. Acad. Sci. Paris, Ser. I, 334 (2002), pp. 1125–1130.
[13] G. ALLAIRE, F. JOUVE AND A.-M. TOADER, *Structural optimization using sensitivity analysis and a level-set method,* J. Comput. Phys., 194 (2004), pp. 363–393.
[14] L. HE, C.-Y. KAO AND S. OSHER, *Incorporating topological derivatives into shape derivatives based level set methods,* J. Comput. Phys., 225 (2007), pp. 891–909.
[15] G. ALLAIRE, F. JOUVE AND A.-M. TOADER, *Structural optimization using topological and shape sensitivity via a level set method,* Contr. Cybernet., 34 (2005), pp. 59–80.
[16] S. AMSTUTZ AND H. ANDRAE, *A new algorithm for topology optimization using a level-set method,* J. Comput. Phys., 216 (2006), pp. 573–588.
[17] M. BURGER, B. HACKL AND W. RING, *Incorporating topological derivatives into level set methods,* J. Comput. Phys., 194 (2004), pp. 344–362.
[18] X. WANG, Y. MEI AND M. Y. WANG, *Incorporating topological derivatives into level set methods for structural topology optimization,* in: T. L. et al. (Eds.), Optimal Shape Design and Modeling, Polish Academy of Sciences, Warsaw, 2004, pp. 145–157.
[19] X. C. TAI AND T. F. CHAN, *A survey on multiple level set methods with applications for identifying piecewise constant functions,* Int. J. Numer. Anal. Model., 1 (2004), pp. 25–47
[20] J. LIE, M. LYSAKER AND X. C. TAI, *A variant of the level set method and applications to image segmentation*, Math. Comput. 75 (2006), pp. 1155–1174.
[21] J. LIE, M. LYSAKER AND X. C. TAI, *A binary level set model and some applications to Mumford-Shah image segmentation,* IEEE Trans. Image Process., 15 (2006), pp. 1171–1181.
[22] J. LIE, M. LYSAKER AND X. C. TAI, *Piecewise constant level set methods and image segmentation,* in Scale Space and PDE Methods in Computer Vision, Lectures notes in Computer Sciences, pp. 573–584, Springer.
[23] J. LIE, M. LYSAKER AND X. C. TAI, *A piecewise constant level set framework,* Int. J. Numer. Anal. Model., 2 (2005), pp. 422–438.
[24] X. C. TAI AND H. W. LI, *A piecewise constant level set method for elliptic inverse problems,* Appl. Numer. Math., 57 (2007), pp. 686–696.
[25] X. C. TAI AND H. W. LI, *Piecewise constant level set method for interface problems, free boundary problems,* Int. Ser. Numer. Math., 154 (2007), pp. 307–316.
[26] P. WEI AND M. Y. WANG, *Piecewise constant level set method for structural topology optimization*, Int. J. Numer. Methods Eng., 78 (2009), pp. 379–402.
[27] S. F ZHU, Q. B. WU AND C. X. LIU, *Variational piecewise constant level set methods for shape optimization of a two-density drum*, J. Comput. Phys., 229 (2010), pp. 5062–5089.
[28] Z. F. ZHANG AND X. L. CHENG, *A boundary piecewise constant level set method for boundary control of eigenvalue optimization problems,* J. Comput. Phys., 230 (2011), pp. 458–473.
[29] J. L. MULLER AND S. SITANEN, *Direct reconstruction of conductivities from boundary measurements,* SIAM J. Sci. Comput., 24 (2003), pp. 1232–1266.
[30] D. GILBARG AND N. S. TRUDINGER, Elliptic Partial Differential Equations of Second Order, Die Grundlehren der Mathematischen Wissenschaften, Vol. 224, Springer, Berlin, 1977.
[31] O. A. LADYZHENSKAYA AND N. N. URAL'TSEVA, Linear and Quasilinear Elliptic Equations, Mathematics in Science and Engineering, Vol. 46, Academic press, New York, 1968.
[32] S. SRINATH AND D. N. MITTAL, *An adjoint method for shape optimization in unsteady viscous flows*, J. Comput. Phys., 229 (2010), pp. 1994–2008.
[33] H. PARK AND H. SHIN, *Shape identification for natural convection problems using the adjoint*

https://doi.org/10.4208/aamm.2012.m42 Published online by Cambridge University Press

variable method, J. Comput. Phys., 186 (2003), pp. 198–211.
[34] S. DURAND, I. CIMRÂK AND P. SERGEANT, *Adjoint variable method for time-harmonic Maxwell equations,* COMPEL: Int. J. Comput. Math. Electrical Electric Eng., 28 (2009), pp. 1202–1215.
[35] P. SERGEANT, I. CIMRÂK, V. MELICHER, L. DUPRÉ AND R. VAN KEER, *Adjoint variable method for the study of combined active and passive magnetic shielding,* Math. Probl. Eng., (2008).
[36] I. CIMRÂK AND V. MELICHER, *Determination of precession and dissipation parameters in the micromagnetism,* J. Comput. Appl. Math., 234 (2010), pp. 2239–2249.
[37] I. CIMRÂK AND V. MELICHER, *Sensitivity analysis framework for micromagnetism with application to optimal shape design of magnetic random access memories,* Inverse Problems, 23 (2007), pp. 563–588.

https://doi.org/10.4208/aamm.2012.m42 Published online by Cambridge University Press